RSC Advances

RSCPublishing

PAPER

View Article Online
View Journal | View Issue

Cite this: *RSC Advances*, 2013, **3**, 10859

Received 1st December 2012, Accepted 28th March 2013

DOI: 10.1039/c3ra40410b

www.rsc.org/advances

High-energy-density materials based on 1-nitramino-2,4-dinitroimidazole†

Jinhong Song,[c] Kai Wang,[a] Lixuan Liang,[a] Chengming Bian[a] and Zhiming Zhou*[ab]

New energetic salts based on 1-nitramino-2,4-dinitroimidazole were successfully synthesized. The salts were fully characterized by ^{1}H, ^{13}C NMR and IR spectroscopy, differential scanning calorimetry (DSC), and elemental analyses. The salts were found to have good physical and detonation properties. The structure of guanidinium salt (**3**) was further confirmed by single-crystal X-ray diffraction. The densities of the energetic salts ranged between 1.70 and 1.93 g cm^{-3} as measured by a gas pycnometer. The detonation pressures and velocities calculated by the EXPLO5 code ranged within 29.3–40.5 GPa and 8370–9209 m s^{-1}, respectively.

Introduction

Energetic salts have attracted considerable attention in recent years because of their roles in the development of modern high-energy-density materials (HEDMs). These salts possess low vapour pressure, high heat of formation, and enhanced thermal stability.[1–4] Numerous nitrogen-containing heterocyclic salts have been investigated by chemists in the USA, Germany, and other countries. A large portion of these salts are based on nitroamino compounds, whose $NHNO_2$ moiety is an important ''explosophore'' that can act as a moderate acid. For example, salts based on 5-nitroaminotetrazole,[5] 3-amino-6-nitroamino-tetrazine,[6a] 4-nitroamino-1,2,4-triazole,[6b] 1-nitroamino-1,2,3-triazole,[6b] 3-azido-5-nitroamino-1,2,4-triazole,[6c] nitroaminodiazido[1,3,5]triazine,[6d] and 4-nitramino-3,5-dinitropyrazole[6e] exhibit excellent performance in terms of impact and friction sensitivity, as well as detonation velocity and pressure. Some bis(heterocyclic) nitroamine energetic salts have also been documented with impressive energetic properties,[1,7a–b] *e.g.*, dihydrazinium ethylene-bridged bis(nitroiminotetrazolate)[7a] (D = 9478 m s^{-1}), ammonium bis[3-(5-nitroimino-1,2,4-triazolate)][1] (D = 9407 m s^{-1}), and 1,2,4,5-tetrazino-3,6-bis(hydrazinium) 1,1′-ethylenebis(oxy)-bis(5-nitroimino-tetrazolate)[7b] (D = 9030 m s^{-1}).

Apart from the aforementioned heterocyclic compounds, imidazole derivatives with more than two nitro groups are potential highly energetic and insensitive explosives.[8] For instance, paired with the same cation, most of 2,4,5-trinitroimidazole (TNI)-based salts have higher densities and energy than 3,4,5-trinitropyrazole-based salts.[9a,b] This characteristic indicates that imidazolate salts would exhibit better detonation properties than pyrazolate salts. The explosive performances of trinitro-substituted imidazoles should approach those of RDX.[9c] However, only TNI-based salts of such type are known. Accordingly, our group is prompted to develop new trinitro-substituted imidazole-based salts whose energy level should be close to that of RDX or even higher. With one C-nitro group transformed into N-nitro and one N–N bond formed by the N-amination of the imidazole ring, the formed 1-nitramino-2,4-dinitroimidazole (NADNI) has higher formation heat than TNI, and may thus be a promising energetic compound. Nitroamino imidazole-based salts are unknown but these salts are expected to exhibit better performances as potential explosives.

In this paper, we report the synthesis, characterization, and detonation performances of NADNI-based energetic salts .

Results and discussion

NADNI was prepared according to literature procedures (Scheme 1).[10,11] Reactions of the potassium salt of NADNI with one equivalent amount of the corresponding chlorides of ammonia, hydrazine, guanidine, aminoguanidine, diaminoguanidine, triaminoguanidine, and 3,4,5-triamino-1,2,4-triazole in H_2O resulted in the formation of salts **1**–**7** (Scheme 2).

All of the salts, which were isolated as powder materials in good yields (>90%), are nonhygroscopic and stable in air. The structures of these salts were confirmed by ^{1}H, ^{13}C NMR and IR spectroscopy, and elemental analysis. Additionally, the structure of guanidinium salt (**3**) was further confirmed by

---

[a] *School of Chemical Engineering and the Environment, Beijing Institute of Technology, Beijing, 100081, P. R. China. E-mail: zzm@bit.edu.cn; Fax: (+86) 10-68918982; Tel: (+86) 10-68918982*

[b] *State Key Laboratory of Explosion Science and Technology, Beijing Institute of Technology, Beijing, 100081, P. R. China*

[c] *School of Chemical Engineering and Material Science, Beijing Institute of Technology, Zhuhai, 519088, P. R. China. E-mail: song_jh@zhbit.com*

† Electronic supplementary information (ESI) available: *Ab initio* computational data. CCDC 885139. For ESI and crystallographic data in CIF or other electronic format see DOI: 10.1039/c3ra40410b

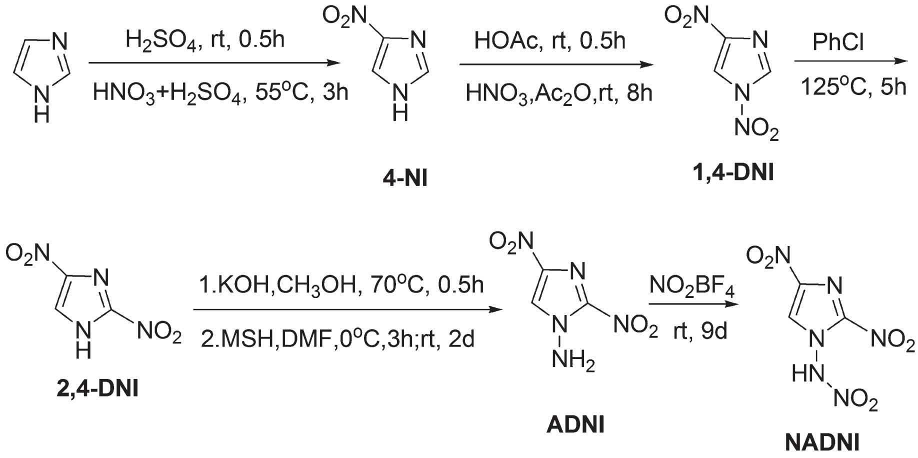

Scheme 1 Synthesis of NADNI.

single-crystal X-ray diffraction. The ^{1}H and ^{13}C NMR spectra were recorded using d_6-DMSO as the locking solvent.

In the ^{1}H NMR spectra, the proton signals of the anion were observed at δ 8.69 ppm, and they were shifted upfield compared with the parent molecule (δ 9.32 ppm). The NH active proton signal of the parent molecule disappeared in the salts spectra.

In the ^{13}C NMR spectra, two signals (δ 123 and 140 ppm) are assigned to the anion (the C4 resonance was not detected according to literature[10,11]). The other signals are associated with the cations. The C5 and C2 peaks (123 and 140 ppm) shifted upfield compared with the parent molecule (126 and 142 ppm). These shifts suggest the anionic properties of NADNI.

In the IR spectra, several main absorption bands at approximately 3150, 1640, 1555, 1501, 1415, 1360, 1330, and 1150 cm^{-1} are attributed to the C–H, N–NO_2 and C–NO_2 bonds of the anions. The intense absorption bands ranging within 3190–3350 cm^{-1} are assigned to the N–H bonds of the nitrogen-rich cations.

Properties of NADNI salts

The melting points (T_m) and decomposition temperatures (T_d) of compounds **1–7** were determined by DSC at a heating rate of 10 °C min^{-1}, respectively. As shown in Table 1, all the salts decomposed without melting. The decomposition temperatures of the NADNI salts fall within the range of 182 °C (**1**) to 194 °C (**7**), which are lower than that of the neutral precursor (T_d = 234 °C).

Density is one of the most important physical properties of energetic compounds. According to the Kamlet–Jacobs equations,[12] the detonation pressure (P) depends on the square of the density, and the detonation velocity (D) is proportional to the density. The densities of all salts were measured with a gas pycnometer (25 °C). As shown in Table 1, the densities of NADNI salts range between 1.70 (**6**) and 1.93 g cm^{-3} (**2**). Particularly, the densities of salts **1**, **2**, **4**, and **6** fall within the

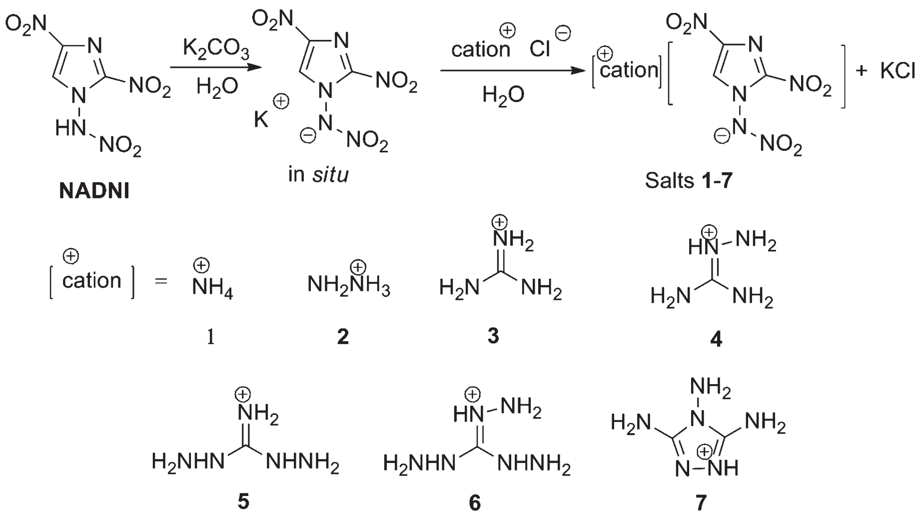

Scheme 2 Synthesis of NADNI-based salts.

Table 1 Properties of energetic salts **1–7**

Salt	T_m[a] (°C)	T_d[b] (°C)	d_{mean}[c] (g cm^{-3})	OB[d] (%)	IS[e] (J)	$\Delta_f H_{cation}$[f] (kJ mol^{-1})	$\Delta_f H_L$[g] (kJ mol^{-1})	$\Delta_f H_{salt}$[h] (kJ mol^{-1})	$\Delta_f U_{salt}$[i] (kJ kg^{-1})	P[j] (GPa)	D[k] (m s^{-1})	T_{del}[l] (K)	V_0[m] (L kg^{-1})	Q_v[n] (kJ kg^{-1})
NADNI	Dec	234	1.80	−7.3	2.5	—	—	278.5	1356.6	35.3	8684	5201	664	−6724
1	Dec	182	1.88	−17.0	4	624.4	504.9	126.6	633.4	37.4	8909	4240	722	−5945
2	Dec	183	1.93	−19.2	12	770.0	500.3	206.8	925.9	40.5	9209	4187	743	−6004
3	Dec	191	1.77	−31.7	40	575.9	475.1	108.0	488.1	30.1	8390	3746	744	−5179
4	Dec	188	1.82	−32.8	35	660.3	473.1	194.3	766.8	33.1	8696	3748	759	−5294
5	Dec	192	1.70	−33.8	>40	769.0	459.3	317.5	1136.9	29.5	8447	3862	782	−5517
6	Dec	193	1.80	−34.8	15	871.5	460.0	418.6	1406..9	34.2	8920	3849	795	−5669
7	Dec	194	1.73	−38.5	13	877.5	452.2	432.5	1389.9	29.3	8370	3881	740	−5364
RDX	Dec	230	1.82	−21.6	7.4	—	—	92.60	417.0	34.8	8748	4207	740	−6129
HMX	Dec	287	1.91	−21.6	7.4	—	—	104.80	357.0	39.2	9059	4135	733	−6060

[a] Melting point. [b] Thermal degradation temperature. [c] Measured density. [d] Oxygen balance. [e] Impact sensitivity. [f] Calculated molar heat of formation of the cation. [g] Calculated molar lattice energy. [h] Calculated heat of formation for the salt. [i] Energy of formation. [j] Calculated detonation pressure (Explo 5.05). [k] Calculated detonation velocity (Explo 5.05). [l] Explosion temperature. [m] Volume of detonation products. [n] Explosion heat.

acceptable range for new high-performance energetic materials (1.8–2.0 g cm^{-3}).[1]

The oxygen balance (OB) is used to indicate the degree to which an explosive can be oxidized. The sensitivity, strength, and brisance of an explosive all somewhat depend on the OB and tend to approach their maximum values as the OB approaches zero. The OBs of the NADNI salts are between −38.5% (**7**) and −17.0% (**1**). Salts **1** and **3** possess better OBs than RDX and HMX.

The impact sensitivities of the synthesized salts are measured using a Fall Hammer on an HGZ-19Z0991 apparatus (5.0 kg drop hammer; 30.0 mg sample). As shown in Table 1, the IS ranges from 4.0 J (**1**) to 40 J (**3** and **5**), most samples are less sensitive than RDX and HMX (7.4 J), and two of them are insensitive compounds.[13]

The heat of formation is another important parameter to be considered in the design of energetic salts. Recently, significant progress has been made in the theoretical prediction of the thermodynamic properties of energetic salts.[14] The heat of formation can be calculated for salts with good accuracy (including the heats of formation of cations and anion, as well as the lattice energy of salts).[14d] In the present study, the heat of formation of the NADNI anions is calculated to be 7.1 kJ mol^{-1} by the Gaussian 03 (Revision D. 01)[15] program suite based on isodesmic reactions (Scheme 4). The values for the cations are available in the literature.[2a,b,16] The heats of formation of the salts are calculated using the Born–Haber energy cycles (Scheme 3). As shown in Table 1, all salts exhibit positive heats of formation and range from 108.0 kJ mol^{-1} (**3**) to 432.5 kJ mol^{-1} (**7**).

The detonation pressures and velocities of the new highly energetic salts, RDX, and HMX are calculated using the program package EXPLO5 version 5.05.[17] As shown in Table 1, the calculated detonation pressures vary between 29.3 (**7**) and 40.5 Gpa (**2**), and the calculated detonation velocities are found between 8370 (**7**) and 9209 m s^{-1} (**2**). In terms of the detonation pressure and velocity, salts **1**, **2**, and **6** are superior to RDX (8748 m s^{-1} and 34.8 GPa, respectively) and NADNI (8684 m s^{-1} and 36.3 GPa, respectively), and salt **2** is superior to HMX (9059 m s^{-1} and 39.2 GPa, respectively). Thus, the salts are competitive energetic materials.

X-Ray crystallography

The X-ray quality crystals of guanidinium salt (**3**) are obtained by slow acetone evaporation at room temperature. The structures are shown in Fig. 1 and the crystallographic data are summarized in Table 2. Salt **3** crystallizes in monoclinic $P2_1/c$ with four molecules in the unit cell and has a calculated density of 1.76 g cm^{-3}. The proton transfer from the NH group of NADNI to guanidine is confirmed in Fig. 2a. The five atoms of the imidazole ring in the NADNI anion are almost coplanar with the dihedral angle of 0° (Table S1, ESI†). The N1–N3 bond

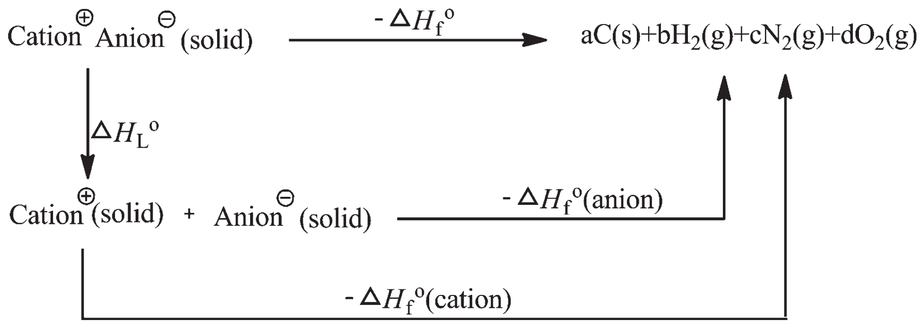

Scheme 3 Born–Haber cycle for the formation for energetic salts.

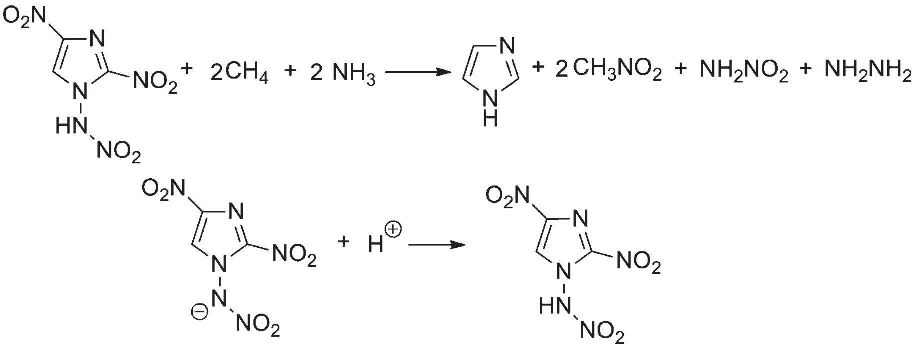

Scheme 4 Isodesmic reactions for calculations of heats of formation.

length (1.403 Å) is close to the N–N single bond length (1.45 Å), and much longer than the N=N double bond length (1.25 Å), which confirms the structure to be nitroamine rather than nitroimine. As shown in Fig. 1b, the dashed lines indicate the strong hydrogen bonding formed between the hydrogen atoms (in the cation and CH group of imidazole) and oxygen atoms (in the nitro groups of the anion). The discrete guanidinium cation and NADNI anion are linked into a 3D network by extensive hydrogen-bonding interactions. Bond lengths: [O1–N4 1.2542(14); O2–N4 1.2507(14); O3–N5 1.2232(15); O4–N5 1.2273(14); O5–N6 1.2237(14); O6–N6 1.2314(15); N1–C1 1.3528(16); N1–C2 1.3721(16); N1–N3 1.4030(15); N2–C2 1.3062(16); N2–C3 1.3534(17); N3–N4 1.3233(15); N5–C2 1.4408(17); N6–C3 1.4351(17); N7–C4 1.3175(19); N7–H7A 0.892(17); N7–H7B 0.891(18); N8–C4 1.3271(18); N8–H8A

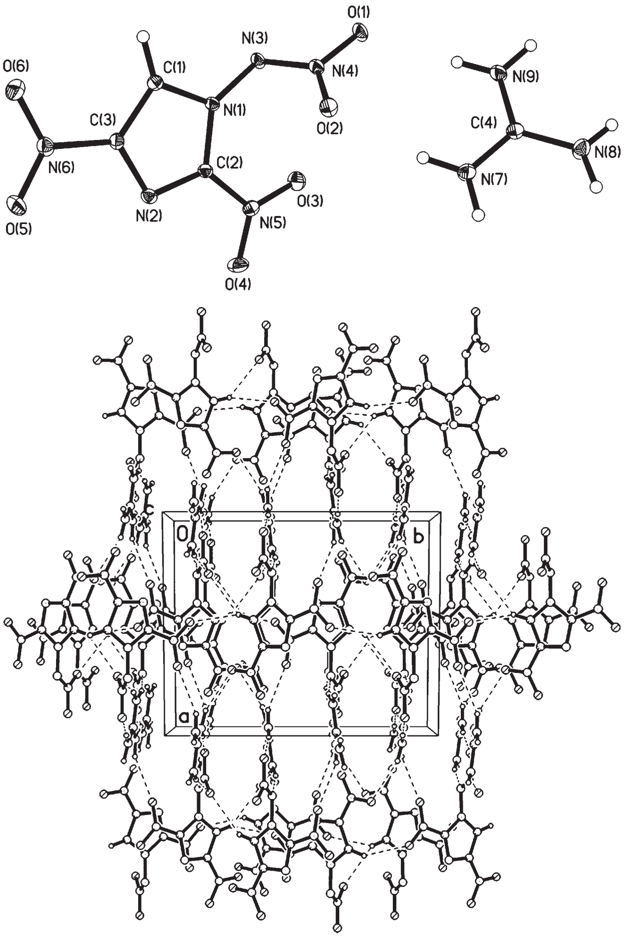

Fig. 1 a) Thermal ellipsoid plot (50%) and labelling scheme for salt **3**. Hydrogen atoms are included but are unlabelled for clarity. b) Ball and stick packing diagram of salt **3** viewed below the *c* axis. Dashed lines indicate strong hydrogen bonding.

Table 2 Crystallographic data for salt **3**

	Salt **3**
Formula	$C_4H_7N_9O_6$
CCDC number	885139
M_r	277.19
Crystal size [mm^{-3}]	0.56 × 0.29 × 0.05
Crystal colour and habit	Yellow platelet
Crystal system	Monoclinic
Space group	$P2_1/c$
a/Å	10.710 (4)
b/Å	13.065 (5)
c/Å	7.574 (2)
Λ(Mo-Kα)[Å]	0.71073
α (°)	90
β (°)	97.613 (5)
γ (°)	90
V/Å^3	1050.3 (7)
Z	4
T/K	153(2)
ρ [mg m^{-3}]	1.76
μ/mm^{-1}	0.16
F_{000}	568
θ/°	2.5 to 29.1
Index ranges	$-14 \leqslant h \leqslant 14$ $-17 \leqslant k \leqslant 17$ $-10 \leqslant l \leqslant 10$
Reflections collected	5096
Independent reflections (R_{int})	2787 (0.033)
Data/restraints/parameters	2040/0/196
GOF on F^2	1.08
$R_1(I > 2\sigma(I))^a$	0.0347
wR_2 ($I > 2d(I)$)	0.0793
R_1 (all data)	0.0558
wR_2 (all data)	0.0729
Largest diff. peak and hole/e Å^{-3}	0.28 and −0.23 e Å^{-3}

[a] $\omega = 1/[\sigma^2(F_o^2) + (0.0472P)^2]$ where $P = (F_o^2 + 2F_c^2)/3$.

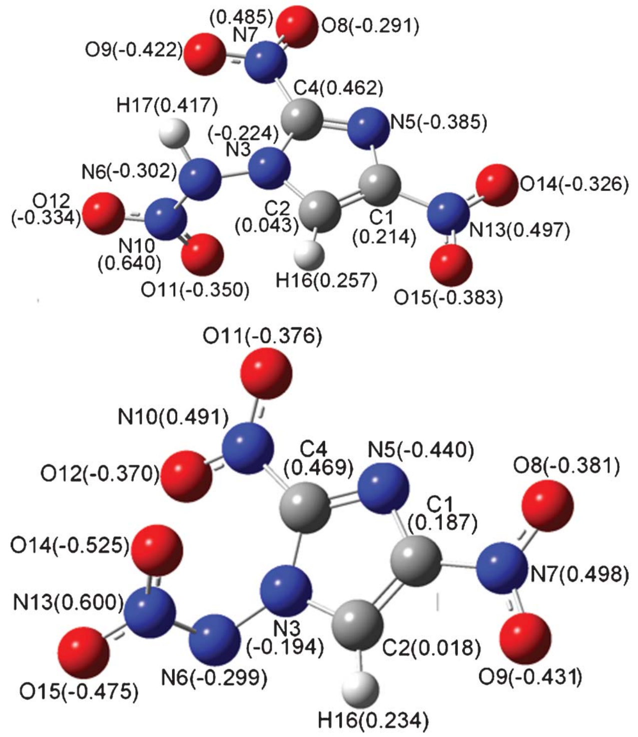

Fig. 2 Optimized structure and charge distribution in NADNI (a) and the anion (b) as found using natural bond orbital analysis (B3LYP/6-311+G(d,p)).

0.864(19); N8–H8B 0.85(2); N9–C4 1.3221(17); N9–H9A 0.858(18); N9–H9B 0.882(19); C1–C3 1.3711(18); C1–H1 0.9500]. Symmetry codes: (i) x, y, z; (ii) −x, y + 1/2, −z + 1/2; (iii) −x, −y, −z; (vi) x, −y − 1/2, z − 1/2.

Theoretical study

Calculations were carried out by the Gaussian 03 (Revision E.01) suite of programs.[14] The geometric optimization of the structures and frequency analyses were carried out by using the B3LYP functional with the 6-31+G**basis set,[18] and single-point energies are calculated at the MP2(full)/6-311++G**level. All of the optimized structures were characterized to be true local energy minima on the potential-energy surface without imaginary frequencies.

Based on the Born–Haber energy cycle (Scheme 3), the heat of formation of a salt can be simplified according to eqn (1), where ΔH_L is the lattice energy of the salt.

$$\Delta H_f^\circ \text{ (ionic salt, 298 K)} = \Delta H_f^\circ \text{ (cation, 298 K)} + \Delta H_f^\circ \text{ (anion, 298 K)} - \Delta H_L \quad (1)$$

ΔH_L can be predicted by the formula suggested by Jenkins *et al.* [eqn (2)],[19] where U_{POT} is the lattice potential energy, and n_M and n_X depend on the nature of the ions M_p^+ and X_q^-, respectively. n_M and n_X are equal to three for monoatomic ions, five for linear polyatomic ions, and six for nonlinear polyatomic ions.

$$\Delta H_L = U_{POT} + [p(n_M/2 - 2) + q(n_X/2 - 2)]RT \quad (2)$$

The equation for the lattice potential energy, U_{POT}, takes the form of eqn (3), where ρ_m is the density (g cm^{-3}), M_m is the chemical formula mass of the ionic material (g), and the coefficients γ (kJ^{-1}mol^{-1}cm) and δ (kJ^{-1}mol^{-1}) are assigned literature values.[19]

$$U_{POT}\ (\mathrm{kJ^{-1}mol^{-1}}) = \gamma\ (\rho_m/Mm)^{1/3} + \delta \quad (3)$$

The subsequent task is the determination of the heats of formation of the cations and anions, which is accomplished using the isodesmic reaction method (Scheme 4). The enthalpy of an isodesmic reaction ($\Delta H_f{}^\circ{}_{298}$) is obtained by combining the MP2(full)/6-311++G**energy difference for the reaction and the scaled zero-point energies (B3LYP/6-31+G**). The heats of formation of the investigated cations and anions can then be readily extracted.

The detonation pressure (P) and detonation velocity (D) are calculated using the program package EXPLO5 version 5.05, in which several parameters are modified. The input is made using the sum formula, energy of formation, and experimental densities measured by a gas pycnometer. The program is based on the chemical equilibrium and the steady-state model of detonation. The program uses the Becker–Kistiakowsky–Wilson's (BKW) equation of state (EOS) for gaseous detonation products, and Cowan–Fickett's EOS for solid carbon.[19–23] The calculation of the equilibrium composition of the detonation products is performed by applying the modified White, Johnson, and Dantzig's free energy minimization technique. The program is designed to enable the calculation of detonation parameters at the CJ point. The BKW equation in the following form is used with the BKW set of parameters (α = 0.5, β = 0.096, κ = 17.56, and θ = 4950) as stated below the equations, where X_i is the molar fraction of ith gaseous product, and k_i is the molar co-volume of the ith gaseous product:

$$pV/\mathrm{R}T = 1 + xe^{\beta x}x = (\kappa \Sigma X_i k_i)/[V(T + \theta)]^\alpha \quad (4)$$

NBO analysis

To gain a better understanding of the structures of the neutral molecule and anion of NADNI, structural optimization and natural bond orbital (NBO) analysis were carried out by Gaussian 03.[15] As shown in Fig. 2a and 2b, all O atoms in the nitro group and the N atoms (N3, N5, and N6) not in the nitro group carry a negative charge, and the other atoms carry a positive charge. In the anion, atom O14 of the nitroamine group carries the most negative charge (−0.525 e) and all O atoms carry more negative charges (−0.525 e − 0.370 e) than the corresponding O atoms (−0.422 e − 0.291 e) in the neutral molecule, which indicates that the negative charge is delocalized over the nitro group to a certain extent.

The charge distribution implies that the more negative O atoms in the anion can form stronger hydrogen bonds with the hydrogen atoms in the cation. The twisted angles between the nitro group and the imidazole ring of the anion are also smaller than those of the neutral molecule. These findings are probably associated with the higher densities and impact sensitivities of the salts than neutral NADNI.

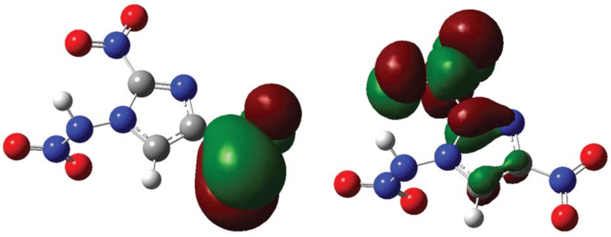

Fig. 3 Highest occupied molecular orbital (left) and lowest unoccupied molecular orbital (right) of NADNI.

The highest occupied molecular orbitals (HOMOs) and lowest unoccupied molecular orbitals (LUMOs) of the neutral molecule and anion of NADNI are shown in Fig. 3 and 4, respectively. In the neutral molecule, the nitro group (N13O14O15) of C–NO_2 occupies the HOMO and the nitro group of the other C–NO_2 occupies the LOMO. In the anion, the nitramine group and a part of the imidazole ring occupy the HOMO and LUMO. Obviously, more atoms occupy the frontier orbitals in the anion than in the neutral molecule. This result indicates that the anion is more reactive and easily attacked by nucleophilic or electrophilic agents.

Conclusions

In summary, new energetic materials of NADNI-based salts were successfully synthesized and fully characterized. The salts exhibit good physical and detonation properties, such as good thermal stabilities, high densities, positive heats of formation, high detonation pressures, and high detonation velocities. The salts also have lower impact sensitivities than the parent. The densities are determined to be 1.70–1.93 g cm^{-3}, and the detonation pressures and velocities are calculated to be 29.3–40.5 GPa and 8370 –9209 m s^{-1}, respectively. The impact sensitivities are measured to be 4–40 J. The detonation properties of salts **1**, **2**, and **6** are superior to that RDX (8748 m s^{-1} and 34.8 GPa, respectively), and salt **2** is superior to HMX (9059 m s^{-1} and 39.2 GPa, respectively). Based on the high density and good detonation properties, these salts show a promising application in the area of HEDMs.

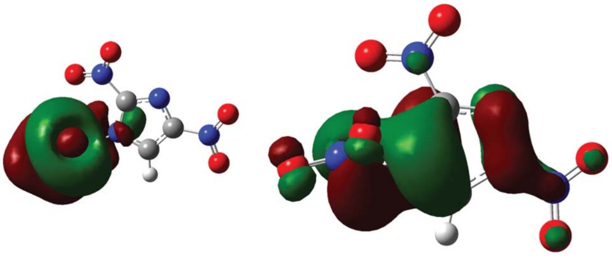

Fig. 4 The highest occupied molecular orbital (left) and lowest unoccupied molecular orbital (right) of NADNI-anion.

Experimental section

Caution! Although none of the compounds described herein have exploded or detonated in the course of this research, these materials should be handled with extreme care using the best safety practices.

General methods

^1H and ^{13}C NMR spectra were recorded on a 400 MHz nuclear magnetic resonance spectrometer operating at 400.18 and 100.63 MHz, respectively. The locking solvent is d_6-DMSO and chemical shifts are reported in ppm relative to TMS. The melting and decomposition points are recorded on a DSC at a scan rate of 10 °C min^{-1}. IR spectra were recorded using a Bruker Alpha with a ATR-Ge device. Densities are measured at room temperature using a Micromeritics Accupyc II1340 gas pycnometer. Elemental analyses were obtained on an Elementar Vario MICRO CUBE (Germany) elemental analyzer.

X-Ray crystallography

Crystals of guanidinium NADNI (NADNI-G) were removed from the flask and covered with a layer of hydrocarbon oil. A suitable crystal was selected, attached to a glass fibre, and placed under a low-temperature nitrogen stream. Data for NADNI-G were collected at 153(2) K using a Rigaku Saturn724 CCD diffractometer equipped with a graphite-monochromatized Mo-Kα radiation (λ = 0.71073 Å) using omega scans. Data collection and reduction were performed and the unit cell was initially refined by the CrystalClear-SM Expert 2.0 r2[24] software. The reflection data were also corrected for the Lp factors. The structure was solved by direct methods and refined by the least squares method on F2 using the SHELXTL-97 system of programs.[25] Structures were solved in the space group $P2_1/c$ for NADNI-G by analysis of systematic absences. In this all-light-atom structure, the value of the Flack parameter did not allow the direction of polar axis to be determined and Friedel reflections were then merged for the final refinement. Details of the data collection and refinements are given in Table 2.

CCDC: 885139 (NADNI-G) contain the supplementary crystallographic data for this paper. The data can be obtained free of charge from The Cambridge Crystallographic Data Centre *via* www.ccdc.cam.ac.uk/data_request/cif.

Reactants: imidazole, ammonium chloride, hydrazine hydrochloride, guanidine hydrochloride (99%), aminoguanidine hydrochloride (98.5%), diaminoguanidine hydrochloride (98.5%) and nitronium tetrafluoroborate (96%) were used as received.

3,4,5-Triamino-1,2,4-triazole hydrochloride, triaminoguanidine hydrochloride were synthesized according to literatures.[26,27]

1-Nitramino-2,4-dinitroimidazole (NADNI)

1-Nitramino-2,4-dinitroimidazole was synthesized according to the literature.[10,11] Pale yellow power. ^1H NMR (400 MHz, acetone-d_6, δ): 6.34 (br, 1H), 8.86 (s, 1H) ppm; ^1H NMR (400 MHz, DMSO-d_6, δ): 6.81 (br, 1H), 9.32 (s, 1H) ppm; ^{13}C NMR (100 MHz, DMSO-d_6, δ): 126.7, 139.4, 142.4 ppm.

General procedure for the synthesis of the salts 1–7

To a solution of NADNI (218 mg, 1.0 mmol) in H_2O (2 mL) was added anhydrous potassium carbonate (0.5 eq). The resulting mixture was stirred at room temperature for 5 min until the evolving CO_2 gas ceased. Followed by adding 1 eq ammonium chloride, hydrazine hydrochloride, guanidine hydrochloride, aminoguanidine hydrochloride, diaminoguanidine hydrochloride, triaminoguanidine hydrochloride and 3,4,5-triamino-1,2,4-triazole hydrochloride, respectively. After stirring at room temperature for 1 h, the yellow precipitate was filtered off, and recrystallized from acetone and ether.

Ammonium 1-nitramino-2,4-dinitroimidazolate salt (1)

Pale yellow powder (212 mg, 90%). ^{1}H NMR (400 MHz, DMSO-d_6, δ): 7.07 (s, 4H), 8.62 (s, 1H) ppm; ^{13}C NMR (100 MHz, DMSO-d_6, δ): 123.16, 141.49 ppm; IR (neat): ν = 3197, 3101, 1640, 1555, 1501, 1414, 1367, 1337, 1307, 1149, 1002, 892, 820, 753, 632 cm^{-1}; elemental analysis (%) calcd for $C_3H_5N_7O_6$: C 15.33, H 2.14, N 41.70; found: C 15.31, H 2.18, N 41.61.

Hydrazinium 1-nitramino-2,4-dinitroimidazolate salt (2)

Yellow powder (246 mg, 98%); ^{1}H NMR (400 MHz, DMSO-d_6, δ): 7.08 (s, 4H), 8.62 (s, 1H) ppm; ^{13}C NMR (100 MHz, DMSO-d_6, δ): 132.1, 53.5 ppm; IR (neat): ν = 3190, 3142, 1555, 1492, 1431, 1367, 1337, 1290, 1149, 1024, 892, 820, 753, 632 cm^{-1}; elemental analysis (%) calcd for $C_3H_6N_8O_6$: C 14.42, H 2.42, N 44.80; found: C 14.39, H 2.40, N 44.69.

Guanidinium 1-nitramino-2,4-dinitroimidazolate salt (3)

Yellow powder (267 mg, 96%); ^{1}H NMR (400 MHz, DMSO-d_6, δ): 6.95 (t, 2H), 8.69 (s, 6H) ppm; ^{13}C NMR (100 MHz, DMSO-d_6, δ): 123.16, 141.50 ppm; IR (neat): ν = 3351, 3272, 3203, 3132, 1648, 1547, 1484, 1416, 1379, 1300, 1150, 988, 886, 818, 753, 634 cm^{-1}; elemental analysis (%) calcd for $C_4H_7N_9O_6$: C 17.33, H 2.55, N 45.48; found: C 17.27, H 2.51, N 45.33.

Aminoguanidinium 1-nitramino-2,4-dinitroimidazolate salt (4)

Yellow powder (278 mg, 95%); ^{1}H NMR (400 MHz, DMSO-d_6, δ): 4.72 (s, 2H), 6.96 (br, 2H), 7.33 (br, 2H), 8.23 (br, 1H), 8.69 (br, 1H) ppm; ^{13}C NMR (100 MHz, DMSO-d_6, δ): 123.26, 141.61, 157.02 ppm; IR (neat): ν = 3383, 3270, 3159, 1648, 1596, 1530, 1484, 1428, 1351, 1215, 1150, 988, 886, 818, 753, 634 cm^{-1}; elemental analysis (%) calcd for $C_4H_8N_{10}O_6$: C 16.42, H 2.76, N 47.94; found: C16.28, H 2.78, N 47.77.

Diaminoguanidinium 1-nitramino-2,4-dinitroimidazolate salt (5)

Yellow powder (277 mg, 90%); ^{1}H NMR (400 MHz, DMSO-d_6, δ): 4.59 (s, 4H), 7.15 (s, 2H), 8.56 (br, 2H), 8.69 (br, 1H) ppm; ^{13}C NMR (100 MHz, DMSO-d_6, δ): 123.61, 139.98, 159.69 ppm; IR (neat): ν = 3354, 3313, 3210, 3132, 1626, 1554, 1484, 1365, 1302, 1269, 994, 955, 818, 753, 632 cm^{-1}; elemental analysis (%) calcd for $C_4H_9N_{11}O_6$: C 15.64, H 2.95, N 50.16; found: C15.43, H 2.90, N 49.95.

Triaminoguanidinium 1-nitramino-2,4-dinitroimidazolate salt (6)

Yellow powder (297 mg, 92%); ^{1}H NMR (400 MHz, DMSO-d_6, δ): 4.49 (br, 6H), 8.60 (br, 3H), 8.69 (br, 1H) ppm; ^{13}C NMR (100 MHz, DMSO-d_6, δ): 123.61, 139.98, 160.54 ppm; IR (neat): ν = 3307, 3204, 3143, 1648, 1554, 1490, 1363, 1337, 1287, 1128, 1067, 1031, 988, 818, 7537, 635 cm^{-1}; elemental analysis (%) calcd for $C_4H_{10}N_{12}O_6$: C 14.91, H 3.13, N 52.17; found: C14.98, H 3.18, N 51.81.

3,4,5-Triamino-1,2,4-triazolium 1-nitramino-2,4-dinitroimidazolate salt (7)

Yellow powder (326 mg, 98%); ^{1}H NMR (400 MHz, DMSO-d_6, δ): 5.54 (s, 2H), 6.87 (br, 4H), 8.69 (br, 1H) ppm; ^{13}C NMR (100 MHz, DMSO-d_6, δ): 123.61, 139.98, 150.25 ppm; IR (neat): ν = 3351, 3291, 3154, 3120, 1642, 1553, 1507, 1484, 1417, 1337, 1302, 1136, 1065, 1024, 889, 819, 753, 633 cm^{-1}; elemental analysis (%) calcd for $C_6H_8N_{12}O_6$: C 18.08, H 2.43, N 50.60; found: C 17.96, H 2.45, N 50.05.

Acknowledgements

The authors gratefully acknowledge the support of Specialized Research Fund for the Doctor Program of Higher Education (No. 20091101110033) and the National Natural Science Fund Project (No. 21172020).

References

1 R. Wang, H. Xu, Y. Guo, R. Sa and J. M. Shreeve, *J. Am. Chem. Soc.*, 2010, **132**, 11904–11905.

2 (*a*) Y. Guo, G. Tao, Z. Zeng, H. Xiang, D. A. Parrish and J. M. Shreeve, *Chem.–Eur. J.*, 2010, **16**, 3753–3762; (*b*) Y. Guo, H. Gao, B. Twamley and J. M. Shreeve, *Adv. Mater.*, 2007, **19**, 2884–2888; (*c*) Y. -H. Joo and J. M. Shreeve, *Angew. Chem., Int. Ed.*, 2009, **48**, 564–567; (*d*) Y.-H. Joo and J. M. Shreeve, *Angew. Chem., Int. Ed.*, 2010, **49**, 7320–7323; (*e*) Y.-H. Joo and J. M. Shreeve, *J. Am. Chem. Soc.*, 2010, **132**, 15081–15090; (*f*) T. M. Klapötke and J. Stierstorfer, *J. Am. Chem. Soc.*, 2009, **131**, 1122–1134.

3 (*a*) J. Song, Z. Zhou, X. Dong, H. Huang, D. Cao, L. Liang, K. Wang, J. Zhang, F. Chen and Y. Wu, *J. Mater. Chem.*, 2012, **22**, 3201–3209; (*b*) J. Song, Z. Zhou, D. Cao, H. Huang, L. Liang, K. Wang and J. Zhang, *Z. Anorg. Allg. Chem.*, 2012, **638**, 811–820; (*c*) H. Huang, Z. Zhou, J. Song, L. Liang, K. Wang, D. Cao, X. Dong and M. Xue, *Chem.–Eur. J.*, 2011, **17**, 13593–13602; (*d*) H. Huang, Z. Zhou, L. Liang, J. Song, K. Wang, D. Cao, C. Bian, W. Sun and M. Xue, *Chem.–Asian. J.*, 2012, **7**, 77–717.

4 (*a*) H. Gao, Y.-H. Joo, D. A. Parrish, T. Vo and J. M. Shreeve, *Chem.–Eur. J.*, 2011, **17**, 4613–4618; (*b*) L. He, G.-H. Tao, D. A. Parrish and J. M. Shreeve, *Inorg. Chem.*, 2011, **50**, 679–685; (*c*) Z. Jalovy, J. Ottis, A. Ruzicka, A. Lycka and N. V. Latypov, *Tetrahedron*, 2009, **65**, 7163–7170; (*d*) Z. Zeng, H. Gao, B. Twamley and J. M. Shreeve, *J. Mater. Chem.*, 2007, **17**, 3819–3826; (*e*) T. M. Klapötke and F. X. Steemann, *Propellants, Explos., Pyrotech.*, 2010, **35**, 114–129; (*f*) M. Göbel, T. M. Klapötke and P. Mayer, *Z. Anorg. Allg. Chem.*, 2006, **632**, 1043–1050.

5 (*a*) L. Wei, J. Zhang, J. Li, T. Zhang and Y. Shu, *New Trends in Research of Energetic Materials, Proceedings of the 14th Seminar*, 2011, **1**, 391–403; (*b*) H. Xue, H. Gao, B. Twamley

and J. M. Shreeve, *Chem. Mater.*, 2007, **19**, 1731–1739; (*c*) N. Fischer, T. M. Klapçtke, F. A. Martin and J. Stierstorfer, *New Trends in Research of Energetic Materials, Proceedings of the 13th Seminar*, 2011, **1**, 113–129.

6 (*a*) H. Gao, R. Wang, B. Twamley, M. A. Hiskey and J. M. Shreeve, *Chem. Commun.*, 2006, 4007–4009; (*b*) Y. Huang, H. Gao, B. Twamley and J. M. Shreeve, *Eur. J. Inorg. Chem.*, 2008, 2560–2568; (*c*) K. Wang, D. A. Parrish and J. M. Shreeve, *Chem.–Eur. J.*, 2011, **17**, 14485–14492; (*d*) Y. Huang, Y. Zhang and J. M. Shreeve, *Chem.–Eur. J.*, 2011, **17**, 1538–1546; (*e*) Y. Zhang, D. A. Parrish and J. M. Shreeve, *Chem.–Eur. J.*, 2012, **18**, 987–994.

7 (*a*) Y.-H. Joo and J. M. Shreeve, *Chem.–Eur. J.*, 2009, **15**, 3198–3203; (*b*) Y.-H. Joo and J. M. Shreeve, *J. Am. Chem. Soc.*, 2010, **132**, 15081–15090.

8 (*a*) S. G. Cho and B. S. Park, *Int. J. Quantum Chem.*, 1999, **72**, 145–154; (*b*) B. M. Rice and J. J. Hare, *J. Phys. Chem. A*, 2002, **106**, 1770–1783; (*c*) J. R. Cho, K. J. Kim, S. G. Cho and J. K. Kim, *J. Heterocycl. Chem.*, 2002, **39**, 141–147; (*d*) R. M. Doherty and R. L. Simpson, *28th International Annual Conference of ICT*, Karlsruhe, 1996, pp. 32.1–32.23.

9 (*a*) Y. Zhang, Y. Guo, Y.-H. Joo, D. A. Parrish and J. M. Shreeve, *Chem.–Eur. J.*, 2010, **16**, 10778–10784; (*b*) H. Gao, C. Ye, O. D. Gupta, J.-C. Xiao, M. A. Hiskey, B. Twamley and J. M. Shreeve, *Chem.–Eur. J.*, 2007, **13**, 3853–3860; (*c*) S. G. Cho and B. S. Park, *Int. J. Quantum Chem.*, 1999, **72**, 145–154.

10 R. Duddu, P. R. Dave, R. Damavarapu, N. Gelbe and D. Parrish, *Tetrahedron Lett.*, 2010, **51**, 399–401.

11 J. R. Cho, K. J. Kim, S. G. Cho and J. K. Kim, *J. Heterocycl. Chem.*, 2002, **39**, 141–147.

12 (*a*) M. J. Kamlet and S. J. Jacobs, *J. Chem. Phys.*, 1968, **48**, 23–35; (*b*) M. J. Kamlet and J. E. Ablard, *J. Chem. Phys.*, 1968, **48**, 36–42; (*c*) M. J. Kamlet and C. Dicknison, *J. Chem. Phys.*, 1968, **48**, 43–49.

13 UN recommendations on the transport of dangerous goods: Impact: Insensitive >40 *J*, less insensitive $\geqslant 35$ *J*, sensitive $\geqslant 4$ *J*, very sensitive $\leqslant 3$ *J*.

14 (*a*) M. W. Schmidt, M. S. Gordon and J. A. Boatz, *J. Phys. Chem. A*, 2005, **109**, 7285–7295; (*b*) K. E. Gutowski, R. D. Rogers and D. A. Dixon, *J. Phys. Chem. B*, 2007, **111**, 4788–4800; (*c*) K. E. Gutowski, J. D. Holbrey, R. D. Rogers and D. A. Dixon, *J. Phys. Chem. B*, 2005, **109**, 23196–23208; (*d*) H. Gao, C. Ye, C. Piekarski and J. M. Shreeve, *J. Phys. Chem. C*, 2007, **111**, 10718–10731; (*e*) X. Zhang, W. Zhu, T. Wei, C. Zhang and H. Xiao, *J. Phys. Chem. C*, 2010, **114**, 13142–13152.

15 M. J. Frisch, G. W. Trucks, H. B. Schlegel, G. E. Scuseria, M. A. Robb, J. R. Cheeseman, J. A. Montgomery Jr., T. Vreven, K. N. Kudin, J. C. Burant, J. M. Millam, S. S. Iyengar, J. Tomasi, V. Barone, B. Mennucci, M. Cossi, G. Scalmani, N. Rega, G. A. Petersson, H. Nakatsuji, M. Hada, M. Ehara, K. Toyota, R. Fukuda, J. Hasegawa, M. Ishida, T. Nakajima, Y. Honda, O. Kitao, H. Nakai, M. Klene, X. Li, J. E. Knox, H. P. Hratchian, J. B. Cross, V. Bakken, C. Adamo, J. Jaramillo, R. Gomperts, R. E. Stratmann, O. Yazyev, A. J. Austin, R. Cammi, C. Pomelli, J. W. Ochterski, P. Y. Ayala, K. Morokuma, G. A. Voth, P. Salvador, J. J. Dannenberg, V. G. Zakrzewski, S. Dapprich, A. D. Daniels, M. C. Strain, O. Farkas, D. K. Malick, A. D. Rabuck, K. Raghavachari, J. B. Foresman, J. V. Ortiz, Q. Cui, A. G. Baboul, S. Clifford, J. Cioslowski, B. B. Stefanov, G. Liu, A. Liashenko, P. Piskorz, I. Komaromi, R. L. Martin, D. J. Fox, T. Keith, M. A. Al-Laham, C. Y. Peng, A. Nanayakkara, M. Challacombe, P. M. W. Gill, B. Johnson, W. Chen, M. W. Wong, C. Gonzalez and J. A. Pople, *Gaussian 03, Revision E.01*, Gaussian, Inc., Wallingford CT, 2004.

16 (*a*) R. Wang, Y. Guo, Z. Zeng, B. Twamley and J. M. Shreeve, *Chem.–Eur. J.*, 2009, **15**, 2625–2634; (*b*) Y. Zhou, C. Yao, R. Ni and G. Yang, *Synth. Commun.*, 2010, **40**, 2624–2632.

17 M. Sućeska, EXPLO5.05 program, Zagreb, Croatia, 2011.

18 R. G. Parr and W. Yang, *Density Functional Theory of Atoms and Molecules*, Oxford University Press, New York, 1989.

19 H. D. B. Jenkins, D. Tudeal and L. Glasser, *Inorg. Chem.*, 2002, **41**, 2364–2367.

20 M. Sućeska, *Mater. Sci. Forum*, 2004, **465–466**, 325–330.

21 M. Sućeska, *Propellants, Explos., Pyrotech.*, 1991, **16**, 197–202.

22 M. Sućeska, *Propellants, Explos., Pyrotech.*, 1999, **24**, 280–285.

23 M. L. Hobbs and M. R. Baer, *Proceedings of the 10th Symposium (International) on Detonation*, ONR 33395-12, Boston, MA, July 12–16, 1993, pp 409.

24 CrystalClear: SM Expert 2.0 r2, An Integrated Program for the Collection and Processing of Area Detector Data, Rigaku Corporation, 2009.

25 G. M. Sheldrick, *SHELXTL-97*, Structure Determination Software Suite, Bruker AXS, Madison WI, USA, 2008.

26 C. Darwich, K. Karaghiosoff and T. M. Klapötke, *Z. Anorg. Allg. Chem.*, 2008, **634**, 61–68.

27 S. Yue and S. Yang, *Chinese J. Synth. Chem.*, 2004, **12**, 164–166.